

# Stratigraphy of the Upper Carboniferous Schooner Formation, southern North Sea: chemostratigraphy, mineralogy, palynology and Sm-Nd isotope analysis

From Earthwise

[Jump to navigation](#) [Jump to search](#)

From: [Carboniferous hydrocarbon resources: the southern North Sea and surrounding onshore areas](#), edited by J. D. Collinson, D. J. Evans, D. W. Holliday, N. S. Jones. Published as volume 7 in the Occasional Publications series of the [Yorkshire Geological Society](#), Copyright [Yorkshire Geological Society](#) 2005.

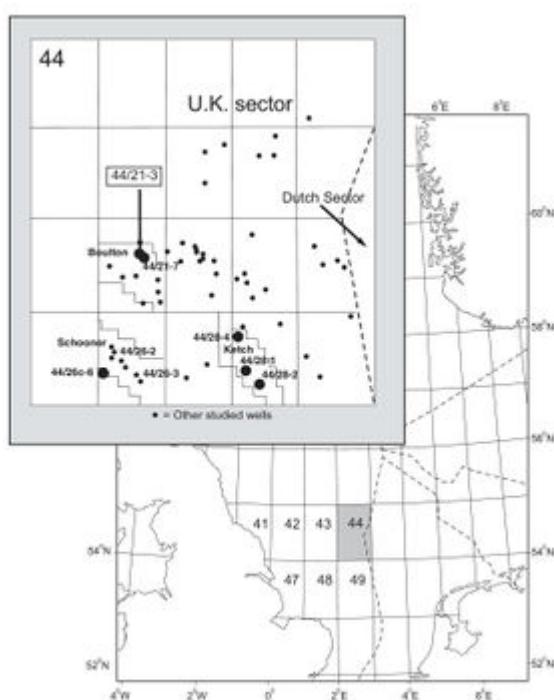


Figure 1 Location of wells and fields referred to in this study. \* = location of other wells that have penetrated the Schooner Formation and which have been the subjects of proprietary chemostratigraphical studies.

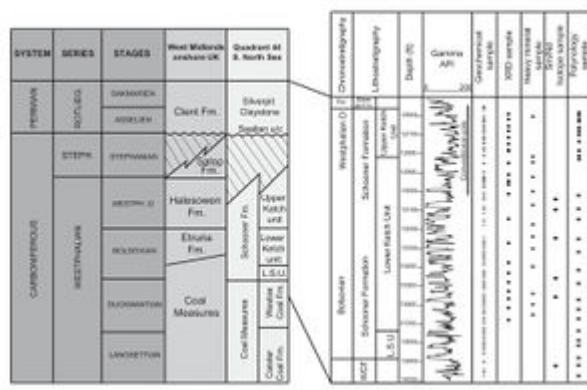


Figure 2 Study interval of well 44/21-3. Quadrant 44 lithostratigraphy from Cameron (1993); West Midlands lithostratigraphy from Besly & Cleal (1997). LSU = Lower Schooner Unit.

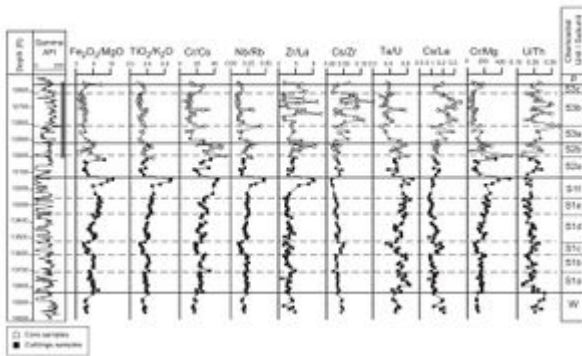


Figure 3 Geochemical profiles for selected element ratios: well 44/21-3.

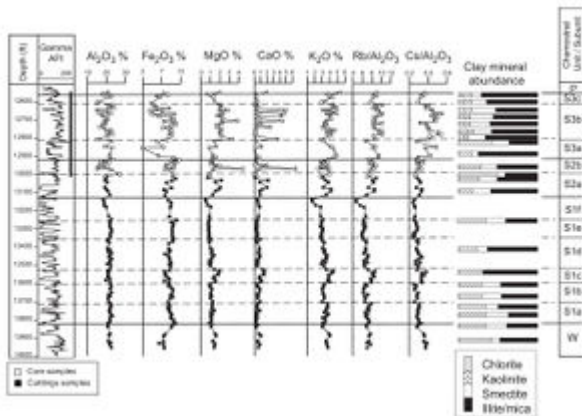


Figure 4 Clay mineralogy related to the abundance of selected major elements in well 44/21-3. The particular elements chosen are those having affinities with clay minerals.

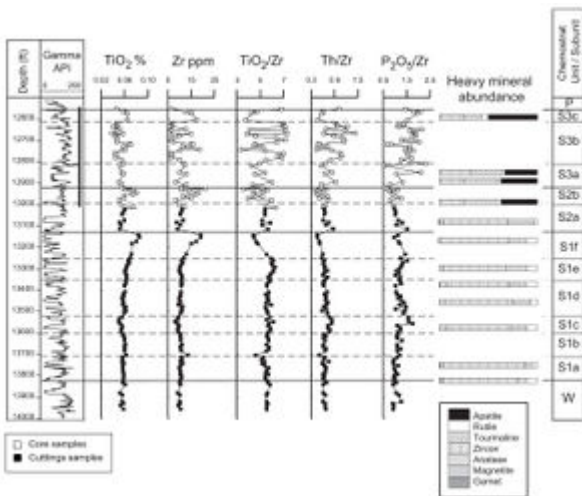


Figure 5 Heavy-mineral assemblages related to the abundance of selected elements and the values of certain element ratios. The particular elements chosen are those having affinities with heavy minerals.

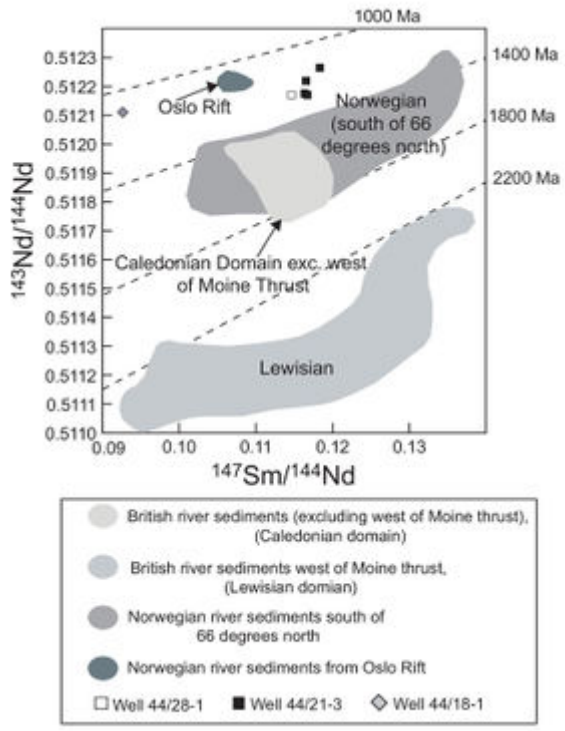


Figure 6 Sm-Nd results for selected mudstone samples from well 44/21-3, 44/28-1 and 44/18-1 (Leng et al. 1999).

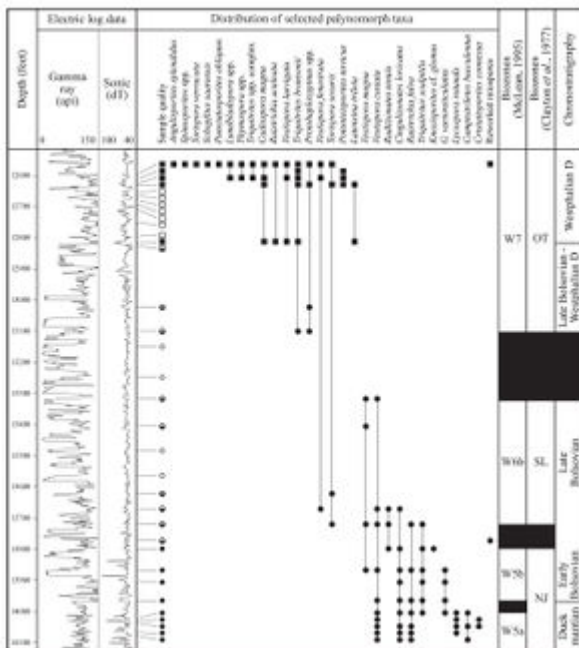


Figure 7 Palynological data: well 44/21-3. Black circle = good sample preservation, half filled circle = moderate sample preservation, no fill = barren.

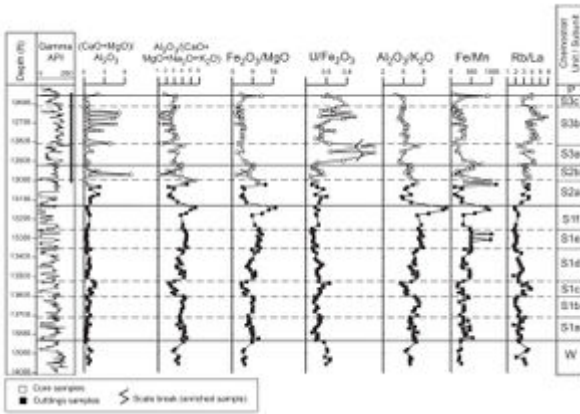


Figure 8 Profiles of geochemical palaeopedology parameters. The profiles are constructed from mudstone data.

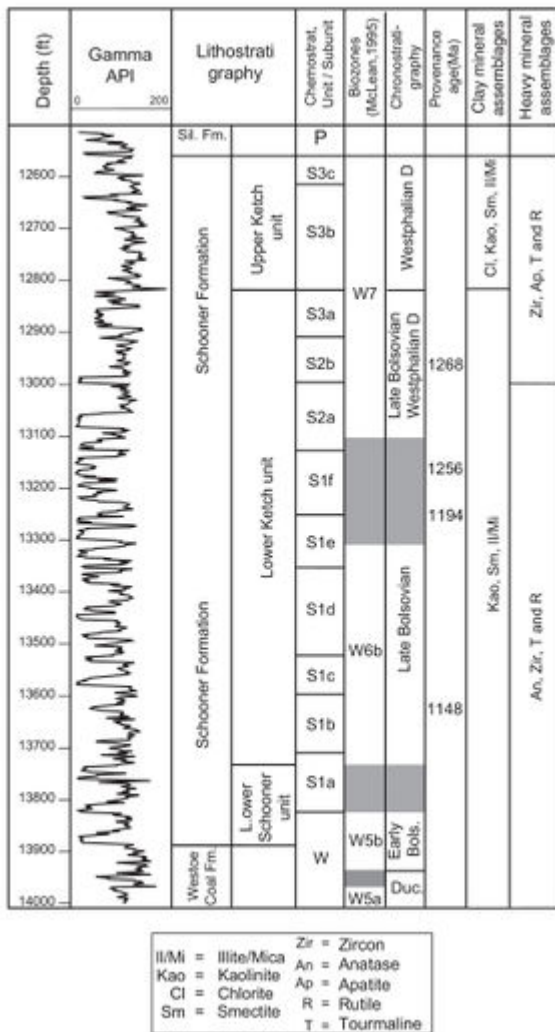


Figure 9 Revised stratigraphy for well 44/21-3 based on the multidisciplinary approach.

Sample type	Depth (ft)	Chemostrat. unit/sub-unit	Chlorite/corrensite			
			illite/mica	Smectite	Kaolinite	(%)
core	12575	S3c	71	12	11	6
core	12609	S3c	64	19	9	8
core	12654	S3b	53	30	9	8
core	12686	S3b	56	29	7	8
core	12729	S3b	60	25	7	8
core	12770	S3b	58	23	7	12
core	12808	S3b	66	21	6	7
core	12818	S3a	36	21	43	—
core	12896	S3a	75	8	17	—
core	12971	S2b	51	20	29	—
core	13013	S2a	41	9	50	—
cuttings	13035	S2a	51	23	26	?trace
cuttings	13097	S2a	59	23	18	?trace
cuttings	13261	S1e	40	24	36	trace
cuttings	13419	S1d	63	13	24	trace
cuttings	13547	S1c	69	—	31	trace
cuttings	13615	S1b	47	24	29	trace
cuttings	13675	S1b	46	24	30	trace
cuttings	13734	S1a	50	15	35	trace
cuttings	13783	S1a	38	27	35	trace
cuttings	13842	W	39	26	35	trace
cuttings	13921	W	47	11	42	trace

Table 1 Clay mineral data: well 44/21-3.

Depth (ft)	Chemostrat. unit/sub-unit	Heavy-mineral assemblages (%)						
		Apatite	Rutile	Tourmaline	Zircon	Anatase	Magnetite	Garnet
12595	S3c	50	7	18	25	—	—	—
12656	S3a	33	3	31	33	—	—	—
12892	S3a	37	3	35	25	—	—	—
12990	S2b	37	4	34	25	—	—	—
13084	S2a	—	3	27	66	3	1	—
13173	S1f	—	11	17	70	2	—	—
13301	S1e	—	10	23	63	4	—	—
13379	S1d	—	11	18	63	7	1	—
13458	S1d	—	7	19	68	5	—	—
13576	S1c	—	10	17	66	7	—	—
13753	S1a	—	4.5	8	83.5	3	—	1
13822	S1a	—	10	9	76	3	—	2

Table 2 Heavy-mineral data: well 44/21-3. Data are reported as % abundances of the heavy-mineral assemblages.

Well	Depth (ft)	Description	Sample type	Sm (ppm)	Nd (ppm)	<sup>147</sup> Sm/ <sup>144</sup> Nd	<sup>143</sup> Nd/ <sup>144</sup> Nd	Prov. age (Ma)
44/21-3	12966	Red sandstone	Cuttings	4	22	0.11670	0.51217	1268
44/21-3	13161	Red sandstone	Cuttings	7	37	0.11636	0.51218	1256
44/21-3	13267	Red siltstone	Cuttings	8	42	0.11653	0.51222	1194
44/21-3	13613	Grey mudstone	Cuttings	10	50	0.11834	0.51226	1148
44/18-1	12409	Not defined	Core	1	8	0.09265	0.51211	c. 1100
44/28-1	13618	Not defined	Core	3	18	0.11464	0.51217	c. 1250

Table 3 Sm-Nd isotopic data: wells 44/21-3, 44/18-1 and 44/28-1; well 44/18-1 and well 44/28-1 data from Leng et al. (1999).

	Unit S3	Unit S2	Unit S1	Unit W
Unit S3	31	0	0	0
Correctly classified (%)	100.0	0.0	0.0	0.0
Unit S2	0	18	1	0
Correctly classified (%)	0.0	94.7	5.3	0.0
Unit S1	1	1	51	7
Correctly classified (%)	1.7	1.7	85.0	11.7
Unit W	0	0	1	6
Correctly classified (%)	0.0	0.0	14.3	85.7
Correctly classified (%)	90.6			

DFA was undertaken on just the mudstone geochemical data. The test assesses whether the chemostratigraphical units and sub-units identified from graphical analysis can also be distinguished statistically. Arabic numerals in horizontal rows refer to numbers of analyzed samples assigned to each chemostratigraphical unit and sub-unit.

Table 4 Results of discriminant-function analysis: well 44/21-3.

□

## Contents

- [1 Stratigraphy of the Upper Carboniferous Schooner Formation, southern North Sea: chemostratigraphy, mineralogy, palynology and Sm-Nd isotope analysis](#)
- [2 Summary](#)
- [3 Introduction](#)
- [4 1. Geological setting](#)
- [5 2. Materials and methods](#)
  - [5.1 2.1 Chemostratigraphy](#)
  - [5.2 2.2 Clay mineral assemblages](#)
  - [5.3 2.3 Sandstone bulk mineralogy](#)
  - [5.4 2.4 Heavy-mineral assemblages](#)
  - [5.5 2.5 Palynology](#)
  - [5.6 2.6 Sm-Nd isotope analysis](#)
- [6 3. Data and interpretations](#)
  - [6.1 3.1 Stratigraphical zonation of the Schooner Formation](#)
    - [6.1.1 3.1.1 Unit W \(sample depths 13841.9 ft to 13956.7 ft\)](#)
    - [6.1.2 3.1.2 Unit S1 \(sample depths 13143.0 ft to 13832.0 ft\) Corresponds to the Lower Schooner Unit and much of the Lower Ketch Unit of Cameron \(1993\).](#)
      - [6.1.2.1 Sub-unit S1a \(sample depths 13723.8 ft to 13832.0 ft\)](#)
      - [6.1.2.2 Sub-unit S1b \(sample depths 13605.9 ft to 13713.9 ft\)](#)
      - [6.1.2.3 Sub-unit S1c \(sample depths 13536.7 ft to 13595.8 ft\)](#)
      - [6.1.2.4 Sub-unit S1d \(sample depths 13359.6 ft to 13526.9 ft\)](#)
      - [6.1.2.5 Sub-unit S1e \(sample depths 13261.2 ft to 13349.7 ft\)](#)
      - [6.1.2.6 Sub-unit S1f \(sample depths 13143.0 ft to 13251.3 ft\)](#)
    - [6.1.3 3.1.3 Unit S2 \(sample depths 12919.1 ft to 13113.5 ft\)](#)
      - [6.1.3.1 Sub-unit S2a \(sample depths 13013.0 ft to 13113.5 ft\)](#)
      - [6.1.3.2 Sub-unit S2b \(sample depths 12919.1 ft to 13002.1 ft\)](#)
    - [6.1.4 3.1.4 Unit S3 \(sample depths 12561.0 ft to 12905.5 ft\)](#)
      - [6.1.4.1 Sub-unit S3a \(sample depths 12818.1 ft to 12905.5 ft\)](#)
      - [6.1.4.2 Sub-unit S3b \(sample depths 12625.9 ft to 12807.7 ft\)](#)
      - [6.1.4.3 Sub-unit S3c \(sample depths 12561.0 ft to 12618.1 ft\)](#)

- [6.1.5 3.1.5 Unit P \(sample depth 12552.5 ft\)](#)
- [7 4. Discussion](#)
  - [7.1 4.1 Validation of the chemostratigraphical zonation](#)
  - [7.2 4.2 Geochemistry and mineralogy](#)
  - [7.3 4.3 Palaeoclimate and palaeoenvironments](#)
  - [7.4 4.5 Implications for future exploration](#)
- [8 5. Conclusions](#)
- [9 Acknowledgements](#)
- [10 References](#)

## **Stratigraphy of the Upper Carboniferous Schooner Formation, southern North Sea: chemostratigraphy, mineralogy, palynology and Sm-Nd isotope analysis**

By T. J. Pearce, D. McLean, D. Wray, D. K. Wright, C. J. Jeans, E. W. Mearns

From: Pages 165–182 of *Carboniferous hydrocarbon geology: the southern North Sea and surrounding onshore areas*, edited by J. D. Collinson, D. J. Evans, D. W. Holliday, N. S. Jones. Published as volume 7 in the Occasional Publications series of the Yorkshire Geological Society, © Yorkshire Geological Society 2005.

### **Summary**

The continental, predominantly redbed sequences of the Upper Carboniferous Schooner Formation (“Barren Red Measures”) from the southern North Sea are a significant gas reservoir, but, as they are largely devoid of microfossils, interwell correlations are difficult. The stratigraphy of the formation is re-evaluated by applying a multidisciplinary approach, which includes chemostratigraphy, mineralogy, palynology, Sm-Nd isotopes, petrophysics and sedimentology, to well 44/21-3, as it has encountered a thick, relatively complete section through the Schooner Formation. The formation is divided into three chemostratigraphical units (S1, S2 and S3) and eleven sub-units on the basis of variations in the mudstone and sandstone data, these variations being linked to changes in provenance, depositional environment and climate. The chemostratigraphical zonation is compared with the biostratigraphical zonation of the same section – heavy-mineral data confirm the sediment source, and Sm-Nd isotope data provide a provenance age for the well 44/21-3 interval. The correlation potential of the new stratigraphical framework is tested on several scales, using data acquired from other southern North Sea wells and from Upper Carboniferous strata of the English Midlands.

### **Introduction**

Seismic and petrophysical data, in conjunction with lithostratigraphy and biostratigraphy, are often employed to establish the stratigraphy of many well sections. Together they can erect reliable interwell correlations for fluvial and alluvial redbed sequences, but cannot always produce the required resolution for detailed stratigraphical modelling. Moreover, the occurrence of thick monotonous successions of sandstones and mudstones with repetitive petrophysical characteristics and no obvious seismic reflectors compounds correlation difficulties. Stone & Moscariello (1999) and Moscariello (2000) have encountered such problems with the Schooner Formation and have attempted to refine its stratigraphy, the formation comprising a significant reservoir play in Quadrants 44 and 49 of the UK southern North Sea.

Different stratigraphical techniques have been applied previously to barren redbed sequences: for example, palaeomagnetism (Hauger et al. 1994), heavy-mineral studies (Mange-Rajetzky 1995, Morton 1985, 1991, Morton & Hallsworth 1994, Morton & Hurst 1995) and isotopic techniques (Dalland et al. 1995, Mearns 1988, Mearns et al. 1989). Unfortunately, their success is limited by a requirement for core material, dependency on a specific lithology and relatively large sample volumes. Consequently, attention has switched to chemical stratigraphy, or chemostratigraphy (Pearce et al. 1999), which characterizes sedimentary rock sequences based on stratigraphical variations in their major-element and trace-element geochemistry. The technique needs only very small samples (0.25g–5g), can be applied to any lithology (Pearce 1991, Pearce & Jarvis 1992a, 1992b, 1995, Pearce et al. 1999, 2005, Ratcliffe et al. in press) and is not restricted by sample type (core samples, cuttings, side-wall core samples and outcrop samples are all suitable). Moreover, chemostratigraphy can provide independent stratigraphical frameworks for redbed fluvial and alluvial well sections (Racey et al. 1995, Preston et al. 1998, Pearce et al. 1999).

Over the past few years, chemostratigraphy has been commonly applied to many redbed Carboniferous well sections in the southern North Sea. Pearce et al. (2005) describe the chemostratigraphical zonation of the Schooner Formation in well 44/21-3 ([Figure 1](#)), which is regarded as the chemostratigraphical reference well for the formation. The zonation has also been recognized in well sections through comparable successions in the Schooner and Boulton fields, thus allowing interwell correlations to be made, although not every chemostratigraphical subunit is identified. This work has demonstrated that variations in sediment geochemistry need to be related to mineral distributions and abundances, facies and potential changes in climate and provenance.

This paper summarizes the results and conclusions of a multidisciplinary study on the Schooner Formation in well 44/21-3. As well as chemostratigraphy, the study includes data acquired from clay-mineral analysis, heavy-mineral analysis, petrography and palynology. Used together, these techniques corroborate the stratigraphical variations in geochemistry recognized over the formation and also furnish information regarding provenance, the age of the formation and changes in depositional environments and climate.

## 1. Geological setting

The Upper Carboniferous in the southern North Sea is made up of three formations ([Figure 2](#)). The sandy coal measures of the Caister Coal Formation are restricted to the northern part of the southern North Sea and are overlain by grey argillaceous coal measures of the Westoe Coal Formation. Above these lies the Schooner Formation (or “Barren Red Measures”), which consists of late Duckmantian to early Bolsovian grey sandy coal measures, followed by Bolsovian red silty mudstones and sandstones (Leeder & Hardman 1990, Besly et al. 1993, Cameron 1993). The formation includes fluvial-channel sandstones and fine-grained delta-plain and alluvial overbank deposits. The sandstones probably were deposited in incised fluvial channels and are sometimes multi-storey, with individual sandbodies possibly having shoestring forms and poor lateral continuity normal to palaeoflow. The fine-grained sediments accumulated as soils, as well as in marshes and lakes when the alluvial plain was waterlogged. Subsidence-related rises in the water table resulted in the deposition of alluvial or lacustrine sediments, whereas periods of uplift led to the incision of fluvial channels, the formation of well drained soils and the sub-aerial weathering of originally grey floodplain deposits (Besly et al. 1993, Cameron 1993, Collinson et al. 1993, Mijnsen 1997).

Significant erosion associated with the Saalian unconformity locally has removed Schooner Formation sections, resulting in Permian successions immediately overlying either the Caister Coal or Westoe Coal formations. Yet relatively thick Schooner Formation sequences are preserved in the axes of northwest–southeast trending Variscan synclines in the Silver Pit Basin area, although such



sequences are either thin or absent over the crests of the intervening anticlines (Leeder & Hardman 1990, Cameron et al. 1992, Bailey et al. 1993).

Well 44/21-3 is located in the Boulton field ([Figure 1](#)) and has penetrated 1350 ft of Schooner Formation deposits ([Figure 2](#)), which represents one of the thickest and most complete sections of the formation encountered so far in the UK sector of the southern North Sea. Indeed, Cameron (1993) regarded this section as one of the reference sections for the Schooner Formation. In the well, the formation consists of grey sandy coal measures assigned to the “Lower Schooner Unit”, which are overlain by the primary redbeds of the Ketch Member ([Figure 2](#)). This member is divided into a “Lower Ketch Unit”, comprising relatively sandy redbeds without caliches and an “Upper Ketch Unit” that consists of interbedded grey and red silty mudstones with thin coals, caliches, limestones and sandstones. Besly et al. (1993) stated that these grey beds yielded a late Duckmantian micro-flora, and gamma-ray log correlations between well 44/21-3 and other wells show that most of the redbeds (= Lower Ketch Unit) in the UK southern North Sea wells are therefore Bolsovian in age. Comparisons with Westphalian sequences in the Dutch sector indicate the presence of younger (Westphalian D) redbeds that do not correlate with the main redbed successions in the Silver Pit Basin. However, Besly (1995) was able to differentiate two redbed successions in the Silver Pit Basin area, equating the upper mudstone-dominated succession with the latest Bolsovian to Westphalian D Upper Ketch Unit.

The base of the Ketch Member is defined by “... the lowest horizon of primary red clays” (Cameron 1993: 22) and “... is commonly close above the highest coal seam of the Schooner Formation”. The boundary has no distinctive e-log break, so careful lithological analysis is recommended for its recognition (Cameron et al. 1993). Although Besly et al. (1993) have demonstrated that dependence on colour for the recognition of this boundary is unreliable, Cameron (1993) maintained a distinction between the primary and secondary redbeds. In contrast, the lower boundary of the Etruria Formation, the onshore equivalent of the Lower Ketch Unit, is conventionally placed at the base of any consistently reddened strata (Bridge et al. 1998). Sometimes the top of the Westoe Coal Formation is positioned to coincide with the highest coal seam imaged on seismic, but, because the Lower Schooner Unit may also contain coals, reliance on this criterion may result in the erroneous placement of the base of the Schooner Formation. The conformable base of this latter formation is marked by abrupt downward decreases in the abundance and thickness of sandstones, so is placed at the base of the lowest clean sandstone (Cameron 1993). It is difficult to pick consistently, although in well 44/21-3 the base of the Schooner Formation is put at 13884.3 ft to coincide with the base of the first thick clean sandstone encountered above the coal measures section.

Thin red mudstone beds of the Permian Silverpit Formation overlie the Schooner Formation in well 44/21-3. The boundary between them is the Saalian unconformity, which is marked by a thin, pebbly conglomerate and is placed at 12558 ft.

## **2. Materials and methods**

Several analytical techniques have been applied to the samples from the Schooner Formation and the overlying and underlying strata of well 44/21-3 and neighbouring wells, including well 44/21-7 ([Figure 1](#)).

### **2.1 Chemostratigraphy**

Two hundred and thirty-seven samples have been analyzed by ICP-OES and ICP-MS techniques. This total comprises 117 mud-stones (44 core samples and 73 cuttings samples) and 15 sandstone core samples from well 44/21-3 ([Figure 2](#)), along with 56 mudstone cuttings samples from well

44/26c-6 and 49 sandstone core samples from well 44/21-7 (Pearce et al. 2005) to provide additional data on sandstones and to test the correlation potential of the zonation. Sampling concentrated on mudstones rather than sandstones, as mudstones are usually fairly well preserved in the cuttings and have more regular element distributions that remain relatively consistent over wide areas (Cullers 1995). Furthermore, the laterally extensive overbank mudstones of the Schooner Formation have better correlation potential than the areally restricted shoestring sandbodies (Stone & Moscariello 1999). Mudstone samples have been collected from throughout the Schooner Formation, from the uppermost part of the underlying Westoe Coal Formation and from the basal part of the overlying Silverpit Formation (Figure 2). Sandstone samples have been collected from the upper two-thirds of the Schooner Formation (i.e. the Lower and Upper Ketch units).

## 2.2 Clay mineral assemblages

The <2µm fractions of 22 mudstone samples (Figure 2) from well 44/21-3 have been subjected to XRD analysis to determine their clay mineralogy, following the methodology of Jeans (1995).

## 2.3 Sandstone bulk mineralogy

Point-counting is the easiest way to determine sandstone bulk mineralogy. However, point-counting formed part of an earlier proprietary sedimentological study on the well 44/21-3 core interval conducted by a third party; so, to avoid data duplication, only brief qualitative examinations of the available sandstone thin sections have been undertaken. The thin sections and original point-count data relate to sandstones from the Upper Ketch Unit and the upper part of Lower Ketch Unit. Accordingly, to gain some insight into the mineralogy of the underlying sandstones (S1 = Lower Ketch and Lower Schooner units of Cameron 1993), thin sections from these sandstones in well 44/21-7, which lies very close (<0.5km) to well 44/21-3 (Figure 1), have been examined, but again, the examinations were of necessity only brief and qualitative, and no point-counting has been undertaken by the authors. However, the original point-count data relating to these thin sections have been released to the authors.

## 2.4 Heavy-mineral assemblages

Twelve sandstone samples (Figure 2) from well 44/21-3 have been subjected to heavy-mineral analysis, following the methodology of Jeans et al. (1993); the resultant data are used to aid the interpretation of the geochemical data and to provide information on provenance. They are corroborated and supplemented by data from Morton et al. (2005) that have been acquired from the Schooner Formation, Westoe Coal Formation and Caister Coal Formation encountered in wells 44/26-3 (Schooner field), plus wells 44/28-1, 44/28-2 and 44/28-4 (Ketch field; Figure 1).

**Table 1 Clay mineral data: well 44/21-3.**

Sample type	Depth (ft)	Chemostrat. unit/sub-unit	Illite/mica	Smectite	Kaolinite	Chlorite/corrensite
(%)						
core	12575	S3c	71	12	11	6
core	12609	S3c	64	19	9	8
core	12654	S3b	53	30	9	8
core	12686	S3b	56	29	7	8
core	12729	S3b	60	25	7	8
core	12770	S3b	58	23	7	12
core	12808	S3b	66	21	6	7

core	12818	S3a	36	21	43	-
core	12896	S3a	75	8	17	-
core	12971	S2b	51	20	29	-
core	13013	S2a	41	9	50	-
cuttings	13035	S2a	51	23	26	?trace
cuttings	13097	S2a	59	23	18	?trace
cuttings	13261	S1e	40	24	36	trace
cuttings	13419	S1d	63	13	24	trace
cuttings	13547	S1c	69	-	31	trace
cuttings	13615	S1b	47	24	29	trace
cuttings	13675	S1b	46	24	30	trace
cuttings	13734	S1a	50	15	35	trace
cuttings	13783	S1a	38	27	35	trace
cuttings	13842	W	39	26	35	trace
cuttings	13921	W	47	11	42	trace

## 2.5 Palynology

Palynology is the standard biostratigraphical technique used to subdivide and correlate southern North Sea Carboniferous well sections (McLean & Murray 1996, McLean & Davies 1999).

Experience shows that palynomorph assemblages recovered from the grey coal measures usually are well preserved and diverse, whereas any from the redbeds tend to be poorly preserved and sparse. Additional controls on the quality and usefulness of palynomorph assemblages are imposed by, *inter alia*, the sample types available (McLean & Davies 1999). However, meticulous sampling of the finer-grained redbed lithologies followed by careful preparation to achieve total dissolution of relatively large amounts of rock material can result in the recovery of moderate- to high-quality assemblages.

Thirty-four core samples and cuttings collected from the grey and redbeds in well 44/21-3 have been analyzed (Figure 2). The samples yielded good-quality assemblages, although 50 per cent of the redbed samples have no palynomorphs.

## 2.6 Sm-Nd isotope analysis

Four samples from well 44/21-3 have been subjected to Sm-Nd isotope analysis. These are subsamples from cuttings and they include mudstones and sandstones. Sample preparation and analysis followed the methodology applied by Faure (1986) and Mearns (1988).

## 3. Data and interpretations

With respect to the various analytical techniques used to establish a multidisciplinary stratigraphical zonation for the Schooner Formation, only the most important findings of each technique are summarized below. Pearce et al. (2005) present the results and conclusions of a detailed chemostratigraphical investigation on the well 44/21-3 study interval; only the variations in the key element ratio values are employed herein to highlight the chemostratigraphical zonation (Figure 3), the ratios including  $\text{Fe}_2\text{O}_3/\text{MgO}$ ,  $\text{TiO}_2/\text{K}_2\text{O}$ ,  $\text{Cr}/\text{Cs}$ ,  $\text{Nb}/\text{Rb}$ ,  $\text{Zr}/\text{La}$ ,  $\text{Ta}/\text{U}$  and  $\text{Cs}/\text{La}$ . Data acquired by the other techniques are presented as follows: clay-mineral data (Figure 4, Table 1), heavy-mineral data (Figure 5 and Table 2), Sm-Nd isotopic data (Figure 6 and Table 3) and palynology data (Figure 7). For brevity, the major elements are given just as chemical symbols rather than oxides from this point onwards. Furthermore, all geochemical ratios are Al ratios unless stated otherwise.

### 3.1 Stratigraphical zonation of the Schooner Formation

As geochemical data have been obtained from the entire Schooner Formation in well 44/21-3 (plus overlying and underlying strata), the data acquired by the other techniques are related to the chemostratigraphical zonation for the formation, which is divided into three chemostratigraphical units (units S1, S2 and S3) and eleven sub-units (Pearce et al., 2005, and [Figure 3](#)). The underlying strata (Westoe Coal Formation) are assigned to unit W and the overlying strata (Silverpit Formation) are assigned to unit P.

**Table 2 Heavy-mineral data: well 44/21-3. Data are reported as % abundances of the heavy-mineral assemblages.**

Depth (ft)	Chemostrat. unit/sub-unit	Apatite	Rutile	Tourmaline	Zircon	Anatase	Magnetite	Garnet
12595	S3c	50	7	18	25	-	-	-
12856	S3a	33	3	31	33	-	-	-
12892	S3a	37	3	35	25	-	-	-
12990	S2b	37	4	34	25	-	-	-
13084	S2a	-	3	27	66	3	1	-
13173	S1f	-	11	17	70	2	-	-
13301	S1e	-	10	23	63	4	-	-
13379	S1d	-	11	18	63	7	1	-
13458	S1d	-	7	19	68	5	-	-
13576	S1c	-	10	17	66	7	-	-
13753	S1a	-	4.5	8	83.5	3	-	1
13822	S1a	-	10	9	76	3	-	2

**Table 3 Sm-Nd isotopic data: wells 44/21-3, 44/18-1 and 44/28-1; well 44/18-1 and well 44/28-1 data from Leng et al. (1999).**

Well	Depth (ft)	Description	Sample type	Sm (ppm)	Nd (ppm)	$^{147}\text{Sm}/^{144}\text{Nd}$	$^{143}\text{Nd}/^{144}\text{Nd}$	Prov. age (Ma)
44/21-3	12968	Red sandstone	Cuttings	4	22	0.11670	0.51217	1268
44/21-3	13161	Red sandstone	Cuttings	7	37	0.11636	0.51218	1256
44/21-3	13267	Red siltstone	Cuttings	8	42	0.11653	0.51222	1194
44/21-3	13613	Grey mudstone	Cuttings	10	50	0.11834	0.51226	1148
44/18-1	12409	Not defined	Core	1	8	0.09265	0.51211	c. 1100
44/28-1	13618	Not defined	Core	3	18	0.11464	0.51217	c. 1250

#### 3.1.1 Unit W (sample depths 13841.9 ft to 13956.7 ft)

**Defining criteria (of base):** The base of the unit lies somewhere below the study interval.

**Geochemical attributes:** Unit W is characterized by low Fe ratio values and relatively high Mg and Na ratio values.

The base of S1 above is defined by sudden downhole reductions in the Fe/Mg, Ta/U, Cr/MgO and Cr/Cs values, as well as increases in the U/Th and Cs/La values ([Figure 3](#)), irrespective of the colour

of the lithology. In addition, unit W has lower Mg, Na, Cr, Nb, Zr, Hf, La and Ce ratios than S1 (Pearce et al. 2005). Sandstone geochemistry: No analyzed samples assigned to this unit.

**Clay mineralogy:** High and equal amounts of illite/mica and kaolinite (c. 40%), plus moderate amounts of smectite and traces of chlorite ([Figure 4](#); [Table 1](#)).

**Heavy-mineral assemblages:** No heavy-mineral data are available for this unit, although Morton et al. (2005) present data from nearby wells. In wells 44/28-2 and 44/28-1, sandstones from the Cleaver Formation (as defined by Besley 2002 and Moscariello et al. 2003) and which is equivalent to a sandstone-rich sequence from the uppermost Westoe Coal Formation) contain abundant zircon, tourmaline, rutile and Cr-spinel, along with minor anatase. This assemblage is broadly comparable with those encountered in the Ketch Member sandstones. Furthermore, the tourmalines found in these sandstones have similar grain chemistry signatures to those from the Ketch Member sandstones, which themselves contain few tourmalines derived from granitic and Al-rich metasedimentary terrains. Occasional sandstone samples from the Cleaver Formation have abundant tourmalines of granitic origin, along with distinctive low CZi values and high ATi values (defined in Morton et al. 2005), which show that these sandstones were derived from more than one source.

**Palynology:** All the analyzed samples assigned to this unit are cuttings and so may contain caved material. Nevertheless, the identification of the homotaxial first appearances downhole of several biostratigraphically important taxa provides recognition of an early Bolsovian to late Duckmantian sequence. These datums are related to the biozones of McLean (1995) and Clayton et al. (1977) in [Figure 7](#). The first appearances downhole of *Lycospora rotunda* and *Camptotriletes bucculentus* (at 13966 ft), in association with the base of the epibole of *Triquitrites sculptilis*, indicate the biozone W5a-W5b boundary of McLean (1995). The same palynological changes are seen across the Aegiranum Marine Band at the Bolsovian stratotype, onshore UK (Riley et al. 1985, Owens et al. 1985), in the Netherlands (Van der Laar & Fermont 1989) and in the Ruhr coalfield (Grebe 1962). Thus, the upper limit of biozone W5a lies close to the Duckmantian/Bolsovian boundary, and the Aegiranum Marine Band is placed somewhere in the high gamma interval between 13900 ft and 13948 ft in well 44/21-3. The Duckmantian/Bolsovian boundary ought to be identified by the lowest stratigraphical occurrence of marine macrofauna within unit W, although the absence of core precludes this. However, the boundary has been picked (following convention in such situations) to coincide with the highest gamma ray peak at 13920 ft. Consequently, the "... gamma marker in productive coal measures" of Besly et al. (1993: [Figure 4](#)) represents the Aegiranum Marine Band.

**Age:** Duckmantian to early Bolsovian.

Comments: The clay mineralogy of unit W is very similar to that of S1a, as both sequences were deposited in waterlogged coal swamp or floodplain. However, unit W can be differentiated from S1 by clear differences in geochemistry and palynology.

### **3.1.2 Unit S1 (sample depths 13143.0 ft to 13832.0 ft) Corresponds to the Lower Schooner Unit and much of the Lower Ketch Unit of Cameron (1993).**

Defining criteria (of base): Abrupt downhole reductions in the  $\text{Fe}_2\text{O}_3/\text{MgO}$ ,  $\text{TiO}_2/\text{K}_2\text{O}$ , Cr/Cs, Cr/MgO, Nb/Rb and Ta/U ratios ([Figure 3](#)), along with an increase in Cs/La, Cs/Zr and U/Th ratios.

Geochemical attributes: Unit S1 is characterized by: \* The top of S1 is placed to coincide with abrupt upward decreases in  $\text{Fe}_2\text{O}_3/\text{MgO}$ ,  $\text{TiO}_2/\text{K}_2\text{O}$ , Nb/Rb, Zr/La, Ta/U and Cr/MgO, but increases in Cs/Zr and Cs/La values ([Figure 3](#)).

- Higher  $\text{Fe}_2\text{O}_3/\text{MgO}$ ,  $\text{TiO}_2/\text{K}_2\text{O}$ , Nb/Rb, Zr/La, Ta/U and Cr/MgO than most unit W, S2 and S3

samples.

- Lower Cs/Zr, Cs/La and U/Th values than units W, S2 and S3 samples.
- Increasing upward Fe<sub>2</sub>O<sub>3</sub>/MgO, TiO<sub>2</sub>/K<sub>2</sub>O, Cr/MgO but decreasing Cs/Zr ratios (especially in the upper half of the unit - [Figure 3](#)).

**Sandstone geochemistry:** Using the geochemical “SandClass System” of Herron (1988), the S1 sandstones (from well 44/21-7; see Pearce et al. 2005) are classified geochemically as sublitharenites, with some quartz arenites. The sandstones have relatively high log Si/Al values, which show quartz is abundant, whereas their high Fe/K values point to detrital clay being relatively scarce, with iron being linked to Fe-oxyhydroxides, ferroan dolomite and ankerite cements (confirmed by petrographical data). Relatively high Ca levels also reflect the presence of ferroan dolomite cements, since calcic detrital minerals such as plagioclase feldspar are rare. These sandstones also have high Zr, Hf and La concentrations, probably because zircon and authigenic kaolinite are abundant, and they are mineralogically more mature than the S3 sandstones.

**Sandstone mineralogy:** Based on petrographical data, most of the S1 sandstones are classified as sublitharenites, with subordinate quartz arenites and litharenites (all after McBride 1963). Monocrystalline and polycrystalline quartz are the predominant detrital components, with the abundance of polycrystalline varieties (usually high-grade metamorphic and cataclastic types) increasing in relation to increasing grain size. Only traces of plagioclase feldspar are noted, whereas lithic clasts of schistose and illitic mudstone metasedimentary rocks occur infrequently. Mica is scarce and is usually degraded, with detrital illitic clay being unimportant. Observed heavy minerals include zircon, tourmaline, rutile, ilmenite, leucosene, and possibly spinel and sphene. Common authigenic products are syntaxial quartz overgrowths, dolomite cements and intergranular kaolinite. The dolomite cements often show non-ferroan to ferroan zoning and may have haematitic cores. Kaolinite occurs as verms and booklets, but is rarely illitized. Siderite cement, chlorite (forming grain-coating “rosettes”), traces of barite and sporadic haematitic coats to detrital grains are less common authigenic products.

**Clay mineralogy:** Illite/mica and kaolinite are predominant, smectite is subordinate and only traces of chlorite are recorded (Table 1). However, illite/mica becomes more abundant in the analyzed S1c and S1d mudstones, mostly at the expense of smectite. Kaolinite abundance decreases from unit W up to the top of S1d, whereas illite/mica abundance increases up section to S1c ([Figure 4](#)). The one analyzed mudstone sample from S1c has a somewhat different clay-mineral assemblage, consisting of only illite/mica (69%) and kaolinite (31%), whereas the clay-mineral assemblages of sub-units S1a, S1b and S1e are broadly similar. Heavy-mineral assemblages: Composed mostly of zircon, with subsidiary tourmaline and rutile, minor anatase and rare magnetite and garnet ([Figure 5](#); [Table 2](#)). Zircon abundance decreases upwards through S1, whereas tourmaline contents increase upwards. In addition, Morton et al. (2005) report significant amounts of Cr-spinel in sandstone core samples (S1a-f equivalents) from the Ketch Member encountered in the Ketch and Schooner field wells. However, the absence of this heavy mineral in the well 44/21-3 cuttings is explained by its preferential removal by mechanical degradation during drilling and the return of the cuttings to wellsite (A. Morton, personal communication). Morton et al. (2005) show the analyzed Ketch Member sandstones from nearby wells have similar heavy-mineral assemblages, which confirms S1a-f (= Ketch Member sandstones) have a uniform provenance signature across Quadrants 44 and 49. The same authors also demonstrate that the tourmalines found in the Ketch Member sandstones consist mostly of varieties originating from Al-poor metasedimentary sources (44–60%), with some varieties coming from Al-rich meta-sedimentary sources (28–40%) and a few coming from granitic sources (6–18%). The provenance age of the analyzed Lower Ketch Unit sandstones from well 44/18-1, as shown by zircon geochronology data, provides evidence for them having a Laurentian-Baltican provenance.

**Palynology:** All the analyzed samples assigned to S1 are cuttings and so may contain caved material. Even so, the recognition of the homotaxial first appearances downhole of several biostratigraphically important taxa provide recognition of, and continued stratigraphical subdivision through, a Bolsovian to late Duckmantian sequence. These datums are related to the biozones of McLean (1995) and Clayton et al. (1977) in [Figure 7](#). Of particular importance are the first appearances downhole of the taxa *Vestispora magna* and *V. costata* (at 13317 ft), *Cingulizonates loricatus* and *Radiizonates tenuis* (at 13622 ft) and *Raistrickia fulva* (at 13671 ft). The first appearances downhole of *Grumosporites varioreticulatus* and common *Raistrickia fulva* (at 13799 ft) are associated with the last appearances downhole of *Torispora securis* and *Knoxisporites sp. cf. K. glomus* (at 13720 ft). These latter events are associated with the upper limits of the *Vestispora magna* (IX) biozone of Smith & Butterworth (1967), the *Vestispora magna* (IV) biozone of van Wijhe et al. (1974), the *Microreticulatisporites nobilis* - *Florinites junior* biozone of Clayton et al. (1977) and the W5 biozone of McLean (1995). The upper limits of these biozones are more or less coincident, those relevant to the onshore UK occurring between the horizons of the Shafton and Cambriense Marine Bands (marine-band nomenclature after Ramsbottom et al. 1978). The base of S1 can be identified using palynology by the occurrence a diagnostic assemblage of reworked late Dinantian to Namurian palynomorphs. In summary, however, S1 is assigned to W5b = early Bolsovian, W6b = late Bolsovian ([Figure 7](#)).

**Age:** Bolsovian.

**Sm-Nd data:** Four analyzed mudstone samples from the Lower Ketch Unit have Sm-Nd isotopic provenance ages between 1148-1276Ma. Leng et al. (1999) presented isotopic data for a Schooner Formation sample from well 44/18-1 and a Westoe Coal Formation sample from well 44/28-1. Although precise provenance ages were not given, the  $^{147}\text{Sm}/^{144}\text{Nd}$  and  $^{143}\text{Nd}/^{144}\text{Nd}$  values, and therefore the provenance ages, are similar to those derived for the samples in the present study ([Table 3 3](#); [Figure 6](#)).

The well 44/21-3 data have been compared with an extensive, mainly in-house, isotopic dataset held by Isotopic Ltd, which has been used to constrain the isotopic signatures of the main source areas around the North Sea. Sediments from the Lewisian domain, which are dominant in British rivers west of the Moine Thrust, have a distinct isotopic signature with a provenance age of >2200Ma. In contrast, sediments sourced from Norwegian rivers south of 66°N have provenance ages between 1350Ma and 1800Ma, whereas sediments from the Caledonian domain, which comprise the sediments in the remaining British rivers, have similar provenance ages (e.g. from 1400Ma to 1820Ma). They typically have a narrower range of  $^{147}\text{Sm}/^{144}\text{Nd}$  values (0.107-0.12) than those from the Norwegian domain, e.g. 0.10- 0.135. Samples from rivers draining the Oslo Rift have a distinct isotopic signature ([Figure 6](#)), with  $^{147}\text{Sm}/^{144}\text{Nd}$  values of 0.105- 0.11 and  $^{143}\text{Nd}/^{144}\text{Nd}$  values of 0.51215-0.51225, which signify a provenance age around 1100Ma.

The well 44/21-3 samples have provenance ages ranging from 1148Ma to 1276Ma. [Figure 6](#) shows that these samples plot between the fields defined by the Oslo Rift samples and the southern Norwegian river samples, so the isotopic signature of the Lower Ketch Unit implies that it consists of a mixture of sediment sourced from the two Norwegian provinces to the northeast. Provenance ages decrease with depth in well 44/21-3, which may point to the gradual denudation of the source area, thereby supplying sediments with progressively older provenance ages.

Unit S1 is divided into six sub-units, which are discussed below.

**Sub-unit S1a (sample depths 13723.8 ft to 13832.0 ft)**

**Geochemical attributes:** Geochemically similar to S1b, although with higher K contents, Rb and Cs

ratios ([Figure 4](#)), and generally higher Zr/La ratios, with the top of S1a is defined by upward decreases in the K, Rb and Cs ratio values.

**Clay mineralogy:** The clay mineralogy of samples from S1a and S1b are broadly similar, with high amounts of illite/mica and kaolinite and subordinate abundances of smectite (Table 1). Overall, kaolinite contents are higher in the S1a samples compared to those in S1b, whereas both S1a and S1b samples have much lower illite/mica than S1c ([Figure 4](#)).

**Heavy-mineral assemblages:** Two samples have been analyzed from S1a. The assemblage comprises zircon (76–83.5%; [Table 2](#)), with subordinate amounts of rutile, anatase and tourmaline, plus minor garnet. Apatite and magnetite are absent.

#### **Sub-unit S1b (sample depths 13605.9 ft to 13713.9 ft)**

**Geochemical attributes:** Although S1b is broadly similar to S1a, it differs from S1c by having higher Fe<sub>2</sub>O<sub>3</sub>/MgO, TiO<sub>2</sub>/K<sub>2</sub>O, Cr/Ls, Nb/Rb, Ta/U ratios, which reduce sharply to define the top of S1b ([Figure 3](#)).

**Clay mineralogy:** Similar to that of the upper S1a sample, although smectite is a little more abundant and illite/mica and kaolinite contents are reduced.

**Heavy-mineral assemblages:** No heavy-mineral data are available for this sub-unit.

#### **Sub-unit S1c (sample depths 13536.7 ft to 13595.8 ft)**

**Geochemical attributes:** Sub-unit S1c is geochemically the most distinctive sub-unit in S1, having higher Cs/La, Cs/Zr and U/Th ratios but lower Fe<sub>2</sub>O<sub>3</sub>/MgO, TiO<sub>2</sub>/K<sub>2</sub>O, Cr/Ls, Nb/Rb, Cr/MgO and Ta/U ratios ([Figure 3](#)). The top is defined by abrupt upward decreases in the Cs/La, Cs/Zr ratios, and increases in Fe<sub>2</sub>O<sub>3</sub>/MgO, TiO<sub>2</sub>/K<sub>2</sub>O, Cr/Ls, Nb/Rb, Ta/U ratios.

**Clay mineralogy:** Compared with S1b, illite/mica contents are much greater (69%), whereas smectite is absent. Kaolinite abundance is unchanged.

**Heavy-mineral assemblages:** As in S1a, zircon is the commonest heavy-mineral type (66%; [Table 2](#)), although its abundance is reduced in S1c. In contrast, tourmaline abundance increases from <10% in S1a to 17% in S1c. Anatase abundance is also slightly higher, although rutile abundance remains unchanged ([Table 2](#)). Garnet is absent.

#### **Sub-unit S1d (sample depths 13359.6 ft to 13526.9 ft)**

**Geochemical attributes:** Similar to sub-units S1e and S1f, which together are characterized by upwardly increasing Fe<sub>2</sub>O<sub>3</sub>/MgO, TiO<sub>2</sub>/K<sub>2</sub>O, Cr/Ls, Cr/MgO and Nb/Rb ratio trends (lowest in S1d), but decreasing Cs/Zr ratios (highest in S1d).

The top of this sub-unit is placed to coincide with stepped upward decrease in Cs/La ratios ([Figure 3](#)).

**Clay mineralogy:** Somewhat similar to the S1c assemblage, although illite/mica and kaolinite are slightly less abundant and smectite is recorded again (Table 1).

**Heavy-mineral assemblages:** Comparable to those of S1c ([Table 2](#)).



### **Sub-unit S1e (sample depths 13261.2 ft to 13349.7 ft)**

**Geochemical attributes:** These seem to be transitional between those of S1d and S1f, although the top of the sub-unit is defined by lowest Cs/La ratios in S1 ([Figure 3](#)).

**Clay mineralogy:** Illite/mica abundance is much lower (40%) than in S1d, whereas kaolinite and smectite abundance is greater (Table 1).

**Heavy-mineral assemblages:** Comparable to those of S1c and S1d ([Table 2](#)).

### **Sub-unit S1f (sample depths 13143.0 ft to 13251.3 ft)**

**Geochemical attributes:** Has the highest Cr/Cs and Cr/MgO ratios and the lowest Cs/Zr ratios of S1. The top of few samples of S1f have the highest Fe<sub>2</sub>O<sub>3</sub>/MgO, TiO<sub>2</sub>/K<sub>2</sub>O, Nb/Rb, and Zr/La values encountered throughout S1 interval.

**Clay mineralogy:** No clay-mineral data are available, although the geochemical data suggest the sub-unit has less illite/mica and more kaolinite than S1e.

**Heavy-mineral assemblages:** Comparable to those of S1c to S1e, although zircon abundance is slightly higher ([Table 2](#)).

### **3.1.3 Unit S2 (sample depths 12919.1 ft to 13113.5 ft)**

**Defining criteria (of base):** The base of S2 is marked by sharp stepped reduction in Fe<sub>2</sub>O<sub>3</sub>/MgO, TiO<sub>2</sub>/K<sub>2</sub>O, Cr/Cs and Nb/Rb, Ta/U, Cr/MgO, but an increase in Cs/Zr and Cs/La ratios ([Figure 3](#)).

**Geochemical attributes:** These are to some extent transitional between those of S1 and S3. Fe<sub>2</sub>O<sub>3</sub>/MgO, TiO<sub>2</sub>/K<sub>2</sub>O, Nb/Rb and Ta/U ratios are all consistently higher than S3 samples, and generally lower in S1 samples, especially those from S1f ([Figure 3](#)). In contrast, Cs/Zr, Cs/La and U/Th ratios are typically higher in S2 than in most upper S1 samples. Cr/Cs ratios are much higher than those in S3, and are similar to those in S1. The top of the unit is marked by abrupt upward increases in the Cs/La and Cs/Zr ratios, along with a major reduction in Fe<sub>2</sub>O<sub>3</sub>/MgO, TiO<sub>2</sub>/K<sub>2</sub>O, Cr/Cs, Nb/Rb and Ta/U ratio values.

**Sandstone geochemistry:** Using the geochemical classification scheme of Herron (1988), the S2 sandstones are classified as Fe-sands and sublitharenites (Herron 1988, Pearce et al. 2005); they also have a similar overall bulk geochemical signature to that of the S1 sandstones.

**Sandstone mineralogy:** Overall, most of the S2 sandstones are mineralogically similar to those of S1, although the former contain apatite and some detrital quartz grains have possible anatase rims and quartz overgrowths.

**Clay mineralogy:** The clay-mineral assemblages consist of variable amounts of kaolinite, smectite and illite/mica ([Table 1](#); [Figure 4](#)). Illite/mica is usually most abundant (41-59%), followed by kaolinite (18-50%) and smectite (9-23%).

**Heavy-mineral assemblages:** Two samples from this unit have been analyzed. Unit S2 sandstones have quite diverse heavy-mineral assemblages. One sandstone contains an assemblage similar to those of S1f (e.g. abundant zircon and tourmaline, plus minor rutile and anatase), whereas the other contains apatite- tourmaline-zircon assemblages with minor rutile (Table 2). Palynology: Assemblages recovered from the S2 interval are relatively poor and contain few stratigraphically significant taxa. The presence of *Triquitrites bransonii* and *Protohaploxylinus* spp. suggest a late

Bolsovian to early Westphalian D age.

**Age:** Late Bolsovian to Westphalian D.

Unit S2 is divided into two sub-units, which are discussed below.

**Sub-unit S2a (sample depths 13013.0 ft to 13113.5 ft)**

**Geochemical attributes:** Compared to S1f and S2b above, S2a is characterized by lower  $\text{Fe}_2\text{O}_3/\text{K}_2\text{O}$ ,  $\text{TiO}_2/\text{K}_2\text{O}$ , Cr/Cs and Ta/U ratios ([Figure 3](#)), which all increase upwards, and along with high Cr/MgO enrichments and low U/Th ratio depletions define the top of the sub-unit.

**Clay mineralogy:** Overall, the assemblages are quite variable, with high illite/mica abundances occurring at the base, and kaolinite contents being higher at the top of the sub-unit ([Table 1](#)). Heavy-mineral assemblages: The analyzed S2a sandstone has an assemblage similar to that of S1f, e.g. abundant zircon and tourmaline, plus minor rutile and anatase ([Table 2](#)).

**Sub-unit S2b (sample depths 12919.1 ft to 13002.1 ft)**

**Geochemical attributes:** Higher  $\text{Fe}_2\text{O}_3/\text{K}_2\text{O}$ ,  $\text{TiO}_2/\text{K}_2\text{O}$ , Cr/Cs and Ta/U ratios ([Figure 3](#)) than S2a and S3.

**Clay mineralogy:** Similar to the assemblages from the lower part of S2a (13035–13097 ft), being characterized by common illite/mica (51%) and broadly comparable smectite and kaolinite contents (20% and 29%, respectively; [Table 1](#)).

**Heavy-mineral assemblages:** An important change is recognized in the assemblage from the base of the sub-unit ([Table 2](#); [Figure 5](#)), with apatite being recorded for the first time. Moreover, it is also the predominant heavy mineral in the sandstones of S2b and S3. In addition, tourmaline is more common. On the other hand, zircon is much less abundant and is no longer the most common heavy mineral, anatase is not recorded from S2b and S3, and rutile, although never abundant, is twice as common below S2b ([Table 2](#)).

**3.1.4 Unit S3 (sample depths 12561.0 ft to 12905.5 ft)**

**Defining criteria (of base):** abrupt increases in the Cs/La and Cs/Zr ratios, along with a sharp reduction in  $\text{Fe}_2\text{O}_3/\text{K}_2\text{O}$ ,  $\text{TiO}_2/\text{K}_2\text{O}$ , Cr/Cs and Ta/U ratios ([Figure 3](#)).

**Geochemical attributes:** Unit S3 samples has higher Cs/Zr, Cs/La, Th/Zr and  $\text{P}_2\text{O}_5/\text{Zr}$ , and low  $\text{Fe}_2\text{O}_3/\text{K}_2\text{O}$ ,  $\text{TiO}_2/\text{K}_2\text{O}$ , Cr/Cs, Cr/MgO and Ta/U ratios (Figs 3, 5) compared to S1 and S2 samples. Some samples assigned to this unit have very high Ca, Mg and Mn levels ([Figure 5](#)).

**Sandstone geochemistry:** Using the geochemical classification scheme of Herron (1988), most of the S3 sandstones are classified as litharenites, although those containing abundant detrital clay are classified as Fe-shales, Fe-sands and wackes (Pearce et al. 2005). The S3 sandstones have higher Al and K contents than the S1 sandstones, which shows that they have more detrital clay and mica, plus, to a lesser extent, feldspar. Some sandstones can have high Ca contents, occasionally >4%. The higher Ca contents reflect the presence of dolomitic cements or, in some cases, rip-up clasts of caliche. Plagioclase feldspar is scarce.

**Sandstone mineralogy:** The S3 sandstones are feldspathic litharenites, containing fresh and variably sericitized K-feldspar and plagioclase. Compared with the other sandstones, they have more mica (mostly degraded, although some unaltered muscovite is observed) and clasts of illitic

mudstone, schistose rocks and metasedimentary rocks. Heavy minerals include apatite, zircon, rutile and tourmaline. Traces of anhydrite cement and sporadic siderite cement occur, with intergranular kaolinite being far less common than in the other sandstones. Haematitic patches after early ?pyrite are observed and dolomite cements (variably haematitic and occasionally zoned) are locally extensive and poikilotopic.

**Clay mineralogy:** Distinct from the S1 and S2 assemblages in having abundant illite/mica and relatively common smectite, although in all but the basal samples kaolinite is scarce ([Table 1](#)). However, each sub-unit of S3 has its own slightly different clay-mineral assemblages.

**Heavy-mineral assemblages:** Comparable with the assemblage of S2b (e.g. abundant apatite, tourmaline and zircon, plus minor rutile; [Table 2](#)), yet the assemblages encountered in 3a and 3c do differ slightly.

**Palynology:** Besly et al. (1993: fig. 4) provided a broad palynostratigraphical summary for the Carboniferous section in well 44/21-3, although no details were given. They considered that the uppermost Carboniferous strata, equivalent to S3, belong to the upper part of the *Torispora securis-Torispora laevigata* (SL) biozone of Clayton et al. (1977). However, the present study indicates that these strata are somewhat younger. Diverse palynological assemblages have been recovered from 12595 ft to 12631 ft and 12815 ft to 12825 ft within the core interval, although the intervening interval contained no palynomorphs. Assemblages from both intervals contain (*inter alia*) common monolete taxa including *Thymospora obscura*, *T. pseudothiesennii*, *Punctatosporites* spp., *Laevigatosporites* spp. and *Latosporites globosus*, with the trilete miospore species *Cadiospora magna*, *Raistrickia aculeata* and *Yestispora laevigata* and the monosaccate pollen *Potonieisporites novicus*. Significant numbers of a complex of forms of *Triquitrites* spp. (*T. additus*, *T. bransonii*, *T. crassus*, *T. sp. cf. T. spinosus*), with *Schopfites saarensis* and *Yestispora fenestrata*, suggest comparison with late Westphalian D assemblages from onshore UK sequences, such as Westphalian D to Stephanian assemblages from the Forest of Dean coalfield (Wagner & Spinner 1972) and from the Saar basin (Bhardwaj 1955). The presence of *Angulisporites splendidus* in the upper interval suggests a latest Westphalian D age, although the species has been considered to represent Stephanian strata. Clayton et al. (1977) used its first appearance to define the mid-Cantabrian base of the *Angulisporites splendidus-Latensina trileta* (ST) biozone ([Figure 7](#)). However, the species does occur in the latest Westphalian D of France (Alpern 1959) and Cantabria (Sánchez de Posada et al. 1999) and has also been recorded from the latest Westphalian D to earliest Stephanian *Lobopteris vestitata* macrofloral biozone in the Forest of Dean. It seems that the true stratigraphical distribution of *A. splendidus* remains to be defined, but its first appearance is somewhere in the mid- to late Westphalian D. In well 44/21-3, its co-occurrence with common *Triquitrites* spp., *Schopfites saarensis*, *Spinosisporites* spp. and *Yestispora fenestrata* indicates that the assemblages are no younger than Westphalian D and are best assigned to the *Thymospora obscura-Thymospora thiessennii* (OT) miospore biozone ([Figure 7](#)), rather than to the Stephanian ST biozone. The lower of these two intervals yields a less diverse assemblage, from which *Thymospora* spp. are not recorded, although *Cadiospora magna*, *Latensina trileta* and *Yestispora laevigata* are noted. These forms again indicate the OT biozone of Westphalian D age, although the absence of the complex of *Triquitrites* spp. and *S. saarensis* suggests that this is the lower part of the biozone, representing the early Westphalian D.

**Age:** Westphalian D.

Unit S3 is divided into three sub-units, which are discussed below.

#### **Sub-unit S3a (sample depths 12818.1 ft to 12905.5 ft)**

**Geochemical attributes:** Sub-unit S3a has very low Fe contents ([Figure 4](#)), which are the lowest recorded anywhere over the study interval, with MgO contents being lower than in S3b and S3c ([Figure 4](#)). S3a also has lower Cs/Zr and Ta/U ratios, but higher Cr/MgO ratios than S3b. The top of the sub-unit is defined by an abrupt upward increase in the Fe contents ([Figure 4](#)) and increases in Cs/Zr and Ta/U ratios, along with strong U/Th ratio enrichments ([Figure 3](#)).

**Clay mineralogy:** Kaolinite is more common than in the other two sub-units ([Table 1](#)). The lower analyzed mudstone contains abundant illite/mica (75%) and minor smectite, whereas the upper analyzed mudstone has less illite/mica, more kaolinite and more smectite.

**Heavy-mineral assemblages:** Apatite, tourmaline and zircon are all relatively abundant, plus minor rutile ([Table 2](#)). Apatite is less common and tourmaline is more common here than in S3c.

#### **Sub-unit S3b (sample depths 12625.9 ft to 12807.7 ft)**

**Geochemical attributes:** Characterized by higher Cs/Zr and Cs/La ratios compared to both S3a and S3c ([Figure 3](#)), and erratic but generally higher TiO<sub>2</sub>/Zr ratios ([Figure 5](#)). S3b is also marked by low Cr/MgO ratios, and high Fe<sub>2</sub>O<sub>3</sub> and MgO contents ([Figure 4](#)) and high Mg and Fe ratio values. Another distinctive feature is the common occurrence of localized peaks along the Ca ratio profile covering S3b, which reflect the presence of calcareous horizons. The top of S3b is marked by decreases in the Cs/La and Cs/Zr ratios and a reduction in MgO contents.

**Clay mineralogy:** Illite/mica is predominant, its abundance being fairly consistent throughout the sub-unit, whereas smectite is subordinate, although its abundance gradually increases upwards ([Table 1](#)). On the other hand, kaolinite is a minor component and is far less common than in S3a. However, chlorite is now recorded in appreciable amounts for the first time, having c. 9 per cent average abundance, in contrast to occurring only in trace amounts over the rest of the underlying study interval ([Table 1](#)).

**Heavy-mineral assemblages:** No heavy-mineral data are available for this sub-unit.

#### **Sub-unit S3c (sample depths 12561.0 ft to 12618.1 ft)**

**Geochemical attributes:** Sub-unit S3c has lower Fe<sub>2</sub>O<sub>3</sub> and MgO contents and lower Cs/La and Cs/Zr ratios than S3c. Cr/Cs ratios are higher in S3c.

**Clay mineralogy:** Illite/mica is predominant once again and is slightly more abundant than in S3b. Smectite is subordinate, but with reduced abundance, whereas kaolinite and chlorite are minor components. Kaolinite is a little more abundant than chlorite and slightly exceeds its abundance in S3b. Chlorite abundance, on the other hand, is about the same ([Table 1](#), [Figure 4](#)). Heavy-mineral assemblages: Broadly comparable with those of S3a, although apatite abundance has increased and tourmaline abundance has dropped ([Table 2](#)).

### **3.1.5 Unit P (sample depth 12552.5 ft)**

**Defining criteria (of base):** Upward increases in the Na and K contents ([Figure 4](#); see also Pearce et al. 2005: [Figure 3](#)).

**Geochemical attributes:** The unit is defined from the geochemical characteristics of just one analyzed sample collected from the basal red mudstones of the Silverpit Formation. It has similar characteristics to those of S3b and S3c, but has much higher Na and K ratio values, attributed to

abundant illite/mica and halite. Unit P also possesses lower Ti/K values overall than S1, S2 and S3.

**Sandstone geochemistry:** No analyzed sandstone samples are assigned to this unit.

**Clay mineralogy:** No clay mineral data are available for this unit. Heavy-mineral assemblages: No heavy-mineral data are available for this unit.

**Age:** Permian

Comments. Unlike the Schooner Formation mudstones, the red mudstones of Unit P are often laminated, have reduction spots and lack any traces of pedogenesis. The overall geochemical similarity between units P and S3 may indicate that the Silverpit Formation contains Schooner Formation material that was reworked during erosion associated with the Saalian unconformity.

## 4. Discussion

### 4.1 Validation of the chemostratigraphical zonation

The validity of the chemostratigraphical zonation is assessed statistically by using discriminant-function analysis (DFA). This statistical test determines whether a given classification, such as the chemostratigraphical zonation, of cases (i.e. samples) into groups (chemostratigraphical units) is appropriate (Aitchison 1986). The results of the test show not only whether a particular sample belongs to a specific unit but also the probability of a sample being assigned to any particular unit. DFA has been applied to just the mudstone geochemical dataset, and the results of the test reveal c. 91 per cent of the analyzed samples are correctly classified ([Table 4](#)). Statistically misclassified samples are randomly distributed over the study interval, apart from five S1 samples between 13536 ft and 13585 ft (S1c) that the DFA results show may be better reassigned to Unit W reflecting a temporary return to more waterlogged floodplain conditions.

### 4.2 Geochemistry and mineralogy

Variations in sediment geochemistry are related to differences in mineral content. Determining the mineral affinities of elements, especially the trace elements, in sedimentary rocks can be difficult, but an assessment of the relationships between element concentrations and mineral distributions, combined with element-to-element correlation coefficients and principal component analysis (PCA), allow the probable controls on element distributions and abundance to be established (Pearce et al. 2005). These authors employ PCA to determine element associations within the mudstones, which in turn can be related to mineralogy and grain size, as follows: \* K, Rb and Cs are associated with illite/mica and chlorite ([Figure 4](#)).

- Ca and Mg (with Mn) are associated with carbonate minerals, although in S3, minor amounts of Mg are linked with chlorite.
- Al, Ti, Nb, Ta, Zr, Hf, Cr, the light rare-earth elements (LREEs - La to Sm) and the heavy rare-earth elements (HREEs - Er to Lu) are all broadly associated. Al and the LREEs are linked with Al-oxyhydroxides and kaolinite. Zr levels are controlled primarily by zircon abundance and distribution, whereas Ti, Nb and Ta are chiefly connected with rutile and opaque minerals, but also occur in authigenic anatase and detrital clay. The HREEs tend to be concentrated in heavy minerals such as zircon, but are also found in clay minerals. Cr is associated mainly with Cr-spinel.

Pearce et al. (2005) present further detailed discussions of the relationships between geochemistry and mineralogy in the Schooner Formation sediments.

**Table 4 Results of discriminant-function analysis: well 44/21-3.**

	Unit S3	Unit S2	Unit S1	Unit W
Unit S3	31	0	0	0
Correctly classified (%)	100.0	0.0	0.0	0.0
Unit S2	0	18	1	0
Correctly classified (%)	0.0	94.7	5.3	0.0
Unit S1	1	1	51	7
Correctly classified (%)	1.7	1.7	85.0	11.7
Unit W	0	0	1	6
Correctly classified (%)	0.0	0.0	14.3	85.7
Correctly classified (%)	90.6			

DFA was undertaken on just the mudstone geochemical data. The test assesses whether the chemostratigraphical units and sub-units identified from graphical analysis can also be distinguished statistically. Arabic numerals in horizontal rows refer to numbers of analyzed samples assigned to each chemostratigraphical unit and sub-unit.

### 4.3 Palaeoclimate and palaeoenvironments

When trying to recognize what impact, if any, climate change has had on the geochemistry of the study interval, it is important first to have some understanding of the regional climatic pattern when these sediments were deposited. They, and their onshore Westphalian equivalents in the English Midlands, were probably deposited in broadly similar environments and under the same overall climatic conditions. The onshore Etruria Formation (Duckmantian–Bolsovian) is distinguished by ferruginous palaeosols and kaolinite is the predominant clay mineral (Besly et al. 1993), whereas the overlying Halesowen and Salop formations (Besly & Cleal 1997), of Westphalian D to early Stephanian age, contain caliches, with illite/mica being the main clay mineral, in addition to minor chlorite (Besly et al. 1993). Similar features can be recognized in the equivalent offshore sequences. The mineralogical differences described above are assumed to reflect climatic change, in that the Etruria Formation sediments (= Lower Ketch Unit) were deposited under humid conditions, whereas the Halesowen and Salop formations sediments (= Upper Ketch Unit) accumulated in a more arid environment (Besly 1987, Besly et al. 1993). Moreover, with respect to the onshore late Carboniferous redbeds in the eastern Netherlands and northern Germany, caliches are found in the overbank sediments of Westphalian D age and younger (Besly et al. 1993, Pagnier & Van Tongeren 1996), with chlorite being a characteristic constituent of the detrital clay-mineral suites (Besly et al. 1993). These characteristics may indicate that the climate changed during Westphalian D times, as has also been interpreted from the UK onshore sequences. Indeed, comparable (probably climate-controlled) facies changes have also been recognized in early Westphalian D successions from the Appalachian Basin (Cecil et al. 1985).

In well 44/21-3, grey coaly intercalations from what is the basal part of S3b have yielded a “. . . late Westphalian C palynoflora (upper part of SL zone)” (Besly et al 1993: 729). However, new palynological data presented herein enable a Westphalian D age to be assigned to this interval, which is broadly comparable to the age of the base of the onshore Halesowen Formation (Besly & Cleal 1997). The differences in Lower and Upper Ketch Unit clay mineralogy, which along with the presence of caliches in the latter unit have been used to invoke climate changes, have been confirmed by the mineralogical data acquired during the course of the multidisciplinary study on well 44/21-3. Furthermore, these changes in clay mineralogy and the positions of the caliches can be modelled geochemically. Al/K ratios are highest in S1, where kaolinite is abundant (Figure 4). In contrast, K, Rb and Cs levels are higher in S2 and S3, these units containing common illite/mica

(Figure 4). Ca contents are low in S1, but are appreciably higher in some samples assigned to S2 and S3. Examination of the available core shows that these latter samples come from mudstones containing caliches. Although in some cases high Mg levels can also be associated with caliches, Mg levels are higher overall in S3b and coincide with significant amounts of chlorite being recorded for the first time over the study interval (Table 4). These mineralogical characteristics are consistent with those described by Besly et al. (1993) and therefore support the proposal of climate change. However, interpretation of the geochemical data and the newly acquired mineralogical data implies that this change began during the deposition of the S2 sediments, the upper part of the Lower Ketch Unit.

Climate change is also reflected by the sedimentology of the Schooner Formation. The thick sandstone-rich intervals corresponding to S1d to S1f were deposited on an alluvial fan (Besly 1995) and the predominance of ferruginous palaeosols and kaolinitic mudstones indicate that intense chemical weathering occurred (oxidation and leaching of detrital minerals) under humid climatic conditions. In contrast, the climate became drier during the deposition of units S2 and S3 (latest Bolsovian to Westphalian D time) and lower-energy floodplain sedimentation prevailed, with the more sporadic deposition of sandstones occurring in fluvial channels and minor lacustrine deltas (Besly 1995, 2002). The reduced sedimentation rates and drier climate permitted not only the establishment of more mature palaeosols and caliches but also the preservation of detrital clay minerals in the mudstones. In addition, localized water-table fluctuations occasionally preserved grey mudstones and thin coals.

Retallack (1997) showed how bulk geochemical data can be utilized as an additional means for classifying the various types of palaeosol. Accordingly, several established geochemical palaeopedology parameters have been applied to those mudstones thought to have undergone pedogenesis (Figure 8). The alkalineearth/alumina ratio,  $(Ca+Mg)/Al$ , assesses soil calcification. In non-calcareous soils, ratio values are usually below 2, but can reach 10 in soils containing carbonate nodules. Throughout S1, ratio values rarely exceed 1, and the same is also true for most of the S2 and S3 samples, although some samples from S2 and especially those from S3b have ratio values between 2 and 5. These samples come from mudstones containing pedogenic carbonate nodules.

The alumina/bases ratio,  $Al/(Ca+Mg+Na+K)$ , reflects the accumulation of insoluble products (clay) with respect to the soluble materials ( $Ca^{2+}$ ,  $Mg^{2+}$ ,  $Na^{2+}$  and  $K^{2+}$ ) liberated by hydrolytic weathering. For the deeply weathered soils termed oxisols, ratio values are high and may reach 100, but in most other soils, ratio values are much lower, usually below 2. The average ratio value for S1 (excluding S1c) is 4.0, which is higher than that for S3 (2.7). The average ratio value of S2 (3.3), lies between them. This indicates that intense chemical weathering under well drained conditions occurred during S1 times, except during S1c when more waterlogged conditions return, probably associated with in basin base level. The impact of intense weathering is apparent sporadically throughout S2, but waned in S3 as climatic conditions changed toward a drier regime.

On the basis of all the above ratio values, the S1 mudstones are classed as either ultisols or oxisols (Retallack 1997), which indicates that they suffered relatively severe hydrolytic weathering, whereas the S2 and S3 mudstones are classed as vertisols. Furthermore, the highest ratio values are recorded at the top of S1 and at the S2a/S2b boundary, and thus may reflect breaks in deposition. The alkaline-earth/alumina ratio values for the S1c samples are slightly higher than those for S1b and S1d, whereas the alumina/bases ratio values for this sub-unit are lower. This could well imply the S1c sediments were deposited under environmental conditions somewhat different from those of the other S1 sediments, for instance, possibly slightly different climatic conditions or changes in basin topography and water-table level.

Other geochemical parameters can be used to model palaeoenvironmental conditions. The Al/K ratio

and the Rb/La ratios (Figure 8) can be used to model the proportion of kaolinite versus illite/mica in samples. K and Rb are enriched in illite/mica, whereas Al and La levels are highest in kaolinite. Samples from S1 and S2b exhibit high Al/K ratios but lower Rb/La ratios, indicating that kaolinite formed following intense chemical weathering under well drained conditions. The U/Fe<sub>2</sub>O<sub>3</sub> and Fe/Mn ratio profiles provide an indication of redox conditions with low U/Fe<sub>2</sub>O<sub>3</sub> ratios, but high Fe<sub>2</sub>O<sub>3</sub>/MnO values corresponding to periods of extensive weathering with the formation of Fe-oxyhydroxides developed on oxidizing conditions. In contrast, U/Fe<sub>2</sub>O<sub>3</sub> are highest (Figure 8) in the more poorly drained conditions from unit W and S3.

The preceding discussion demonstrates how sediment composition is greatly influenced by climate. Nonetheless, much more relevant information could be derived if a detailed sedimentological investigation were made on the core interval of well 44/21-3, with particular attention being paid to the pedogenic horizons, as well as a palynofacies study being conducted (Lott 1992, both in Glover & Powell 1996, Besly & Cleal 1997, Bridge et al. 1998), whereas the S1 sediments were sourced from southern Norway. However, uplift of the Variscan front across northern continental Europe resulted in the initiation of a new source area, sediments from which were deposited across central England (e.g. the Halesowen Formation) and the southern North Sea (e.g. S3, = Upper Ketch Unit). This change in provenance appears to be diachronous and can be monitored by palynological data. In well 44/21-3, S3 is Westphalian D in age, but in the English Midlands there is evidence for a provenance change during latest Westphalian C times (Besly & Cleal 1997, Besly 1995). Collinson et al. (1993) noted that the late Westphalian redbeds from Quadrants 52 and 53 to the south and from onshore Lincolnshire have lithic compositions pointing to derivation from a southerly source area (Variscan?) and thus are probably comparable to the Upper Ketch Unit. These sandy redbeds were assigned to the Brig Formation by Cameron (1993). He noted that the Lower Brig Unit, a condensed sequence of Bolsovian- Westphalian D coal measures, is approximately age-equivalent to the Upper Ketch Unit, whereas the overlying primary redbeds of the Upper Brig Unit have comparable E-log characteristics and a similar age to the Halesowen Formation (Besly & Cleal 1997).

#### **4.5 Implications for future exploration**

The study described herein has clearly demonstrated that, if a multidisciplinary approach is applied to the stratigraphy of Schooner Formation, then a detailed stratigraphy can be erected (Figure 9). Similar multidisciplinary approaches are currently being applied by operators across the southern North Sea. In the past, separating the red mudstones of the Silverpit Formation from the reddened mudstones of the Schooner Formation has been difficult when only cuttings are available, the boundary between them corresponding to the top of the Carboniferous (= Saalian unconformity). However, this boundary can now be identified relatively easily and confidently by using geochemical data and clay-mineral data. Furthermore, S1, S2 and S3 can be recognized across the southern North Sea, indicating that they can form the basis of a new subregional correlation framework.

The feldspathic litharenitic sandstones of S3 are of poorer reservoir quality than the sublitharenitic sandstones of S1 and S2, particularly the thicker, porous, sometimes pebbly sandstones occurring over the upper part of S1. The mineralogical differences between the sandstones are reflected by their differing geochemical signatures. Consequently, a better understanding of the Schooner Formation stratigraphy in one or more well sections will enable more confident predictions of where the S1 sandstones of higher reservoir quality may occur, this prediction being confirmed by determining whether the sandstones in question have S1 geochemical signatures.

As the changes in clay mineralogy and sedimentology of S2 and S3 reflect a change in climate, these changes provide what may be regarded as a subregional chemostratigraphical "event". Moreover, the different provenance of the Upper Ketch Unit provides another basis for correlation, although



this may be diachronous over a large area. Pearce et al. (2005) present a sub-regional correlation, based on chemostratigraphy, for wells from the Boulton and Schooner fields. Stone & Moscariello (1999) and Moscariello (2000) utilized chemostratigraphy and pedofacies data to remodel the reservoir zonation for the Schooner field. Chemostratigraphy is also being used to confirm the stratigraphy of TD sections and the depth of the Saalian unconformity in the Hawkley field (Block 44/17), where wells have penetrated the Schooner Formation (Conway et al. 2002).

The multidisciplinary approach has also been used to model the subregional relationship between the Schooner Formation and the underlying coal measures. The base of the formation can be identified using palynological and chemostratigraphical data, and in well 44/21-3 the sandstone assigned to S1a yields a diagnostic assemblage of reworked late Dinantian to Namurian palynomorphs. Experience indicates that this sandstone can be recognized in many well sections from UK Quadrants 44 and 49. Moreover, palynological data confirm that basal samples of S1a are assigned to biozone W6b of Late Bolsovian age, and overlie samples from biozone W5b of the early Bolsovian (Pearce et al. 2005), confirming the presence of an unconformity at the base of the Schooner Formation. The recognition of this unconformity is critical to modelling the extent of reservoirs in both the uppermost coal measures and in the Schooner Formation.

## 5. Conclusions

- The Schooner Formation in well 44/21-3 is proposed as the chemostratigraphical reference section for this formation. On the basis of geochemical variations recognized over the section, it is divided into three chemostratigraphical units (S1, S2 and S3) and eleven sub-units, this zonation being supported by mineralogical and palynological data. The geochemical variations can be recognized from both the mudstone and sandstone geochemical datasets.
- Geochemical variations recognized over the formation in well 44/21-3 reflect a change towards an increasingly arid climate. Furthermore, the integrated approach shows a major change in provenance began in S2, became predominant with the deposition of S3 in well 44/21-3. This change in provenance is comparable to a similar change recognized in the Late Carboniferous sandstones of central England. In addition, Sm-Nd isotopic provenance ages imply that the Lower Ketch Unit sediments were derived from several sources lying to the east and northeast (e.g. southern Norway). However, the Upper Ketch Unit sediments were supplied from a southerly Variscan source.
- The Schooner Formation in well 44/21-3 is Bolsovian to Westphalian D in age. The chemostratigraphical units to which the formation is assigned correspond to the main biostratigraphical intervals (e.g. S1 is equivalent to biozone W6b (late Bolsovian)), whereas units S2 and S3 correspond to biozone W7. The base of the Schooner Formation represents a subregional unconformity. Its position is marked by an abrupt change in mudstone geochemistry and by the occurrence of a thick sandstone containing a diagnostic assemblage of reworked palynomorphs.
- The important geochemical characteristics of the Schooner Formation in well 44/21-3 are also recognized from the same formation in other wells (Pearce et al. 2005), which allows interwell chemostratigraphical correlations to be made. Since these geochemical characteristics are linked to changes in provenance and climate, the chemostratigraphical units should be identified over a wide area, thereby making large-scale interwell correlations possible.

## Acknowledgements

The authors wish to thank ConocoPhillips UK Ltd, plus their respective partners, for access to the sample material and for permission to publish the paper. The work of Lorna Dyer, Department of Earth Sciences, University of Greenwich, is greatly appreciated. The authors thank Dr N. Meadows

and Dr J. Riding for their constructive reviews of the typescript, although the views expressed in this paper are those of the authors alone.

## References

- Aitchison, J. 1986. *The statistical analysis of compositional data*. London: Chapman & Hall.
- Alpern, B. 1959. *Contribution à l'étude palynologique et pétrographique des charbons française*. PhD thesis, l'Université de Paris.
- Bailey, J. B., P. Arbin, O. Daffinoti, P. Gibson, J. S. Ritchie 1993. Permo-Carboniferous plays of the Silver Pit Basin. In *Petroleum geology of northwest Europe: proceedings of the 4th conference*, J. R. Parker (ed.), 707-715. London: Geological Society.
- Besly, B. M. 1987. Sedimentological evidence for Carboniferous and Early Permian palaeoclimates of Europe. *Société géologique du Nord, Annales* 106, 131-43.
- Besly, B. M. 1987. 1995. Stratigraphy of Late Carboniferous redbeds in the southern North Sea and adjoining land areas. Paper presented at "Strati-graphic advances in the offshore Devonian and Carboniferous rocks, UKCS and adjacent onshore areas" conference, Geological Society, London, January 1995.
- Besly, B. M. 1987. 2002. Late Carboniferous redbeds of the UK southern North Sea viewed in a regional context [abstract: pp. 17-20.]. This volume: 225-226.
- Besly, B. M. & C. J. Cleal 1997. Upper Carboniferous stratigraphy of the West Midlands (UK) revised in the light of borehole geophysical logs and detrital compositional suites. *Geological Journal* 32, 85-118.
- Besly, B. M., S. D. Burley, P. Turner 1993. The late Carboniferous "Barren Red Bed" play of the Silver Pit area, southern North Sea. In *Petroleum geology of northwest Europe: proceedings of the 4th conference*, J. R. Parker (ed.), 727-40. London: Geological Society. Bhardwaj, D. C. 1955. The spore genera from the Upper Carboniferous coals of the Saar and their value in stratigraphical studies. *Palaeobotanist* 4, 119-49.
- Bridge, D. McC., J. N. Carney, R. S. Lawley, A. W. A. Rushton 1998. *Geology of the country around Coventry and Nuneaton*. Memoir, Sheet 169, British Geology Survey (England and Wales).
- Cameron, T. D. J. 1993. Carboniferous and Devonian of the southern North Sea. In *Lithostratigraphic nomenclature of the UK North Sea* (vol. 5), R. W. O'B. Knox & W. G. Cordey (eds), 1-93. Nottingham: British Geological Survey.
- Cameron, T. D. J., A. Crosby, P. S. Balson, D. H. Jeffrey, G. K. Lott, J. Bulat, D. J. Harrison 1992. *The geology of the southern North Sea*. United Kingdom Offshore Regional Report, British Geological Survey, Keyworth, Nottingham.
- Cecil, C. B., R. W. Stanton, S. G. Neuzil, R. T. Dulong, L. F. Ruppert, B. S. Pierce 1985. Paleoclimate controls on Late Paleozoic sedimentation and peat formation in the central Appalachian basin. *International Journal of Coal Geology* 5, 195-230.
- Clayton, G., R. Coquel, J. Doubinger, S. Loboziak, B. Owens, M. Streeel 1977. Carboniferous miospores of Western Europe: illustration and zonation. *Mededelingen Rijks Geologische Dienst* 29, 1-72.

- Cleal, C. J., T. K. Dimitrova, E. L. Zodrow 2003. Macrofloral and palynological criteria for recognizing the Westphalian-Stephanian boundary. *Newsletter in Stratigraphy* 39, 181-208.
- Collinson, J. D., C. M. Jones, G. Blackbourn, B. M. Besly, G. M. Archard, A. H. McMahon 1993. Carboniferous depositional systems of the southern North Sea. In *Petroleum geology of northwest Europe: proceedings of the 4th conference*, J. R. Parker (ed.), 677- 87. London: Geological Society.
- Conway, A. M., I. M. Fozdar, R. Ings 2002. CMS III realizing a cluster development of Westphalian B and C/D reservoirs [abstract: p. 23]. Paper presented at "Hydrocarbon resources of the Carboniferous, southern North Sea and surrounding areas" conference, Yorkshire Geological Society, Sheffield, September 2002.
- Cullers, R. L. 1995. The controls on the major- and trace-element evolution of shales, siltstones and sandstones of Ordovician to Tertiary age in the West Mountains region, Colorado, USA. *Chemical Geology* 123, 107-131.
- Dalland, A., E. W. Mearns, J. J. McBride 1995. The application of samarium-neodymium (Sm-Nd) provenance ages to correlation of biostratigraphically barren strata: a case study of the Statfjord Formation in the Gullfaks oil field, Norwegian North Sea. In *Nonbiostratigraphical methods of dating and correlation*, R. E. Dunay & E. A. Hailwood (eds), 201-222. Special Publication 89, Geology Society, London.
- Dolby, G. 1989. *The palynology of the Morien Group, Sydney Basin, Cape Breton Island, Nova Scotia*. Open Report 88/16, Nova Scotia Department of Mines.
- Faure, G. 1986. *Principles of isotope geology*, 2nd edn. New York: John Wiley.
- Glover, B. W. & J. H. Powell 1996. Interaction of climate and tectonics upon alluvial architecture: Late Carboniferous-Early Permian sequences at the southern margin of the Pennine Basin, UK. *Palaeogeography, Palaeoclimatology, Palaeoecology* 121, 13-34.
- Grebe, H. 1962. Zur Verbreitung der Sporen im oberen Westfal B und dem Westfal C des Ruhrkarbons. *Fortschritte in der Geologie von Rheinland und Westfalen* 3, 773-86.
- Hallsworth, C. R. 1992. *Stratigraphic variations in the heavy minerals and clay mineralogy of the Westphalian to Early Permian succession from the Daleswood Farm borehole, and the implications for sand provenance*. Technical Report WH/92/185R, British Geological Survey, Keyworth, Nottingham.
- Hallsworth, C. R., A. C. Morton, J. C. Claoue-Long, C. M. Fanning 2000. Carboniferous sand provenance in the Pennine Basin, UK: constraints from heavy mineral and SHRIMP zircon age data. *Sedimentary Geology* 137, 147-85.
- Hauger, E., R. Lovlie & P. Van Veen 1994. Magnetostratigraphy of the Middle Jurassic Brent Group in the Oseberg oil field, northern North Sea. *Marine and Petroleum Geology* 11, 375-88.
- Herron, M. M. 1988. Geochemical classification of terrigenous sediments using log or core data. *Journal of Sedimentary Petrology* 58, 820-29.
- Jeans, C. V. 1995. Clay mineral stratigraphy in Palaeozoic and Mesozoic redbed facies onshore and offshore UK. In *Dating and correlating biostratigraphically barren strata*, R. E. Dunay & E. A. Hailwood (eds), 31-55. Special Publication 89, Geology Society, London.
- Jeans, C. V., S. J. B. Reed, M. Xing 1993. Heavy-mineral stratigraphy in the UK Trias: Western

Approaches, onshore England and the central North Sea. In *Petroleum geology of northwest Europe: proceedings of the 4th conference*, J. R. Parker (ed.), 609-624. London: Geological Society.

Leeder, M. R. & M. Hardman 1990. Carboniferous geology of the Southern North Sea Basin and controls on hydrocarbon prospectivity. In *Tectonic events responsible for Britain's oil and gas reserves*, R. F. P. Hardman & J. Brooks (eds), 87-105. Special Publication 55, Geology Society, London.

Leng, M. J., B. W. Glover, J. I. Chisholm 1999. Nd and Sr isotopes as clastic provenance indicators in the Upper Carboniferous of Britain. *Petroleum Geoscience* 5, 293-301.

Lott, G. K. 1992. *Petrology and diagenesis of the Upper Carboniferous sandstones from the Daleswood Farm borehole, south Staffordshire*. Technical Report, WH/92/182R, British Geological Survey, Keyworth, Nottingham.

McBride, E. F. 1963. A classification of common sandstones. *Journal of Sedimentary Petrology* 33, 664-9.

McLean, D. 1995. A palynostratigraphic classification of the Westphalian of the southern North Sea Carboniferous Basin. Poster presented at "Stratigraphic advances in the offshore Devonian and Carboniferous rocks, UKCS and adjacent onshore areas" conference, Geological Society, London, January 1995.

McLean, D. & S. J. Davies 1999. Constraints on the application of palynology to the correlation of Euramerican Late Carboniferous clastic hydrocarbon reservoirs. In *Biostratigraphy in production geology*, R. W. Jones & M. Simmons (eds), 201-218. Special Publication 152, Geological Society, London.

McLean, D. & I. Murray 1996. Subsurface correlation of coal seams and interseam sediments using palynology: applications to exploration for coalbed methane. In *Coalbed methane and coal geology*, R. Gayer & I. Harris (eds), 315-25. Special Publication 97, Geological Society, London.

Mange-Rajetzky, M. A. 1995. Subdivision and correlation of monotonous sandstone sequences using high-resolution heavy-mineral analysis, a case study: the Triassic of the Central Graben. In *Nonbiostratigraphical methods of dating and correlation*, R. E. Dunay & E. A. Hailwood (eds), 23-30. Special Publication 89, Geology Society, London.

Mearns, E. W. 1988. A samarium-neodymium isotopic survey of modern river sediments from northern Britain. *Chemical Geology* 73, 1-13.

Mearns, E. W., R. Knarud, N. Reastad, K. O. Stanley, C. P. Stockbridge 1989. A samarium-neodymium isotope stratigraphy of the Lunde and Statfjord formations of the Snorre oil field, northern North Sea. *Geological Society of London, Journal* 146, 217-28.

Mijnssen, F. C. J. 1997. Modelling of sandbody connectivity in the Schooner field. In *Petroleum geology of the southern North Sea: future potential*, K. Ziegler, P. Turner, S. R. Daines (eds), 169-80. Special Publication 123, Geological Society, London.

Morton, A. C. 1985. Heavy minerals in provenance studies. In *Provenance of arenites*, G. G. Zuffa (ed.), 249-77. Dordrecht: Reidel.

Morton, A. C. 1991. Geochemical studies of detrital heavy minerals and their application to provenance studies. In *Developments in sedimentary provenance studies*, A. C. Morton, S. P. Todd,

P. Haughton (eds), 31–45. Special Publication 57, Geological Society, London.

Morton, A. C. & C. Hallsworth 1994. Identifying provenance-specific features of detrital heavy-mineral assemblages in sandstones. *Sedimentary Geology* 90, 241–56.

Morton, A. C. & A. Hurst 1995. Correlation of sandstones using heavy minerals: an example from the Statfjord Formation of the Snorre field, northern North Sea. In *Non-biostratigraphical methods of dating and correlation*, R. E. Dunay & E. A. Hailwood (eds), 23–30. Special Publication 89, Geology Society, London.

Morton, A. C., C. Hallsworth, A. Moscariello 2005. Interplay between northern and southern sediment sources during Westphalian deposition in the Silverpit Basin, southern North Sea. This volume: 135– 146.

Moscariello, A. 2000. Pedofacies in reservoir modelling of low net to gross, barren fluvial sequences (Schooner Formation, Carboniferous SNS). Paper presented at EAGE 62nd Conference and Technical Exhibition, May–June 2000, Glasgow, 1–4.

Moscariello, A. 2003. The Schooner field, Blocks 44/26a and 43/30a, UK southern North Sea. In *The United Kingdom oil and gas fields commemorative millennium volume*, J. Gluyas & H. Hichens (eds), 811–24. Memoir 20, Geological Society, London.

Owens, B., N. J. Riley, M. A. Calver 1985. Boundary stratotypes and new stage names for the Lower and Middle Westphalian sequences in Britain. *Dixième Congrès Internationale de Stratigraphie et de Géologie du Carbonifère, Madrid, 1983, compte rendu*, vol. 4, 461– 72.

Pagnier, H. J. M. & C. H. Van Tongeren 1996. Upper Carboniferous of borehole “De Lutte-6” and evaluation of the Tubbergen Formation in the eastern and southeastern parts of the Netherlands. *Mededelingen Rijks Geologische Dienst* 55, 3–30.

Pearce, T. J. 1991. *The geology, geochemistry, sedimentology and provenance of Late Quaternary turbidites, Madeira Abyssal Plain*. PhD thesis, Kingston Polytechnic.

Pearce, T. J. & I. Jarvis 1992a. The composition and provenance of turbidite sands: Late Quaternary Madeira Abyssal Plain. *Marine Geology* 109, 21–51.

Pearce, T. J. 1992b. Applications of geochemical data to modelling sediment dispersal patterns in distal turbidites: Late Quaternary of the Madeira Abyssal Plain. *Journal of Sedimentary Petrology* 62, 1112– 29.

Pearce, T. J. & I. Jarvis 1995. High-resolution chemostratigraphy of Quaternary distal turbidites: a case study of new methods for the correlation of barren strata. In *Non-biostratigraphical methods of dating and correlation*, R. E. Dunay & E. A. Hailwood (eds), 107– 143. Special Publication 89, Geology Society, London.

Pearce, T. J., B. M. Besly, D. Wray, D. K. Wright 1999. Chemostratigraphy: a method to improve interwell correlation in barren sequences – a case study using onshore Duckmantian/Stephanian sequences (West Midlands, UK). *Sedimentary Geology* 124, 197– 220.

Pearce, T. J., D. Wray, K. Ratcliffe, D. K. Wright, A. Moscariello 2005. Chemostratigraphy of the Upper Carboniferous Schooner Formation, southern North Sea. This volume: 147–164.

Preston, J., A. Hartley, M. Hole, S. Buck, J. Bond, M. Mange, J. Still 1998. Integrated whole-rock

trace-element geochemistry and heavy-mineral chemistry studies: aids to the correlation of continental redbed reservoirs in the Beryl field, UK North Sea. *Petroleum Geoscience* 4, 7-16.

Racey, A., M. A. Love, R. M. Bobolecki, J. N. Walsh 1995. The use of chemical element analysis in the study of biostratigraphically barren sequences: an example from the Triassic of the central North Sea (UKCS). In *Non-biostratigraphical methods of dating and correlation*, R. E. Dunay & E. A. Hailwood (eds), 69-105. Special Publication 89, Geology Society, London.

Ramsbottom, W. H. C., M. A. Calver, R. M. C. Eagar, F. Hodson, D. Holliday, C. J. Stubblefield, R. B. Wilson 1978. *A correlation of Silesian rocks in the British Isles*. Special Report 10, Geological Society, London.

Ratcliffe, K. T., T. J. Pearce, J. Martin, A. D. Hughes, in press. Enhanced reservoir characterization of the Triassic Argilo Greseux Inferieur, Algeria using high resolution chemostratigraphy. *American Association of Petroleum Geologists, Bulletin* 89.

Retallack, G. J. 1997. *A colour guide to palaeosols*. Chichester, England: John Wiley.

Riley, N. J., M. J. Razzo, B. Owens 1985. A new boundary stratotype section for the Bolsopian (Westphalian C) in northern England. *Dixième Congrès Internationale de Stratigraphie et de Géologie du Carbonifère, Madrid, 1983, compte rendu*, vol. 1, 35-44.

Sánchez de Posada, L. C., E. Villa, L. Matínez Chacón, R. M.

Rodríguez, S. Rodríguez, R. Coquel 1999. Contenido paleontológico y edad de la sucesión de Demués (Carbonífero, zona Cantábrica). *Trabajos de geología (Oviedo)* 21, 339-52.

Smith, A. H. V. & M. A. Butterworth 1967. *Miospores in the coal seams of the Carboniferous of Great Britain*. Special papers in palaeontology 1, Palaeontological Association, London.

Stone, G. & A. Moscariello 1999. Integrated modelling of the southern North Sea Carboniferous Barren Red Measures using production data, geochemistry, and pedofacies cyclicity. *Offshore Europe 99, Proceedings, Aberdeen, 1999*, 1-8.

Van de Laar, J. G. M. & W. J. J. Fermont 1989. Onshore Carboniferous palynology of the Netherlands. *Mededelingen Rijks Geologische Dienst* 43, 35-73.

Van Wijhe, O. H., M. J. M. Bless, S. J. Dijkstra 1974. The Westphalian of the Netherlands with special reference to miospore assemblages. *Geologie en Mijnbouw* 53, 259-328.

Wagner, R. H. & E. Spinner 1972. The stratigraphic implications of the Westphalian D macro- and microflora of the Forest of Dean coalfield (Gloucestershire), England. *Proceedings of the International Geological Congress (Montreal, 1972)*, vol. 7, 428-37.

Retrieved from

[http://earthwise.bgs.ac.uk/index.php?title=Stratigraphy\\_of\\_the\\_Upper\\_Carboniferous\\_Schooner\\_Formation\\_southern\\_North\\_Sea:\\_chemostratigraphy,\\_mineralogy,\\_palynology\\_and\\_Sm-Nd\\_isotope\\_analysis&oldid=45616](http://earthwise.bgs.ac.uk/index.php?title=Stratigraphy_of_the_Upper_Carboniferous_Schooner_Formation_southern_North_Sea:_chemostratigraphy,_mineralogy,_palynology_and_Sm-Nd_isotope_analysis&oldid=45616)

Category:

- [Carboniferous hydrocarbon resources: the southern North Sea and surrounding onshore areas](#)

# Navigation menu

## Personal tools

- Not logged in
- [Talk](#)
- [Contributions](#)
- [Log in](#)
- [Request account](#)

## Namespaces

- [Page](#)
- [Discussion](#)

## Variants

## Views

- [Read](#)
- [Edit](#)
- [View history](#)
- [PDF Export](#)

## More

## Search

## Navigation

- [Main page](#)
- [Recent changes](#)
- [Random page](#)
- [Help about MediaWiki](#)

## Tools

- [What links here](#)
- [Related changes](#)
- [Special pages](#)
- [Permanent link](#)
- [Page information](#)

- [Cite this page](#)
- [Browse properties](#)

• This page was last modified on 11 May 2020, at 11:16.

- [Privacy policy](#)
- [About Earthwise](#)
- [Disclaimers](#)

